Fast Degradation of dyes in water using Manganese-Oxide-Coated Diatomite for Environmental Remediation

Trung-Dung Dang,[*a#] Arghya Narayan Banerjee,[*b#] Quang-Tung Tran,[a] and Sudipta Roy[*c]

[a]*School of Chemical Engineering, Hanoi University of Science and Technology, 1st Dai Co Viet, Hai Ba Trung, Hanoi, Vietnam.*

[b]*School of Mechanical Engineering, Yeungnam University, Gyeongsan 712-749, South Korea.*

[c]*Department of Chemical Engineering and Processing, University of Strathclyde, Glasgow, United Kingdom.*

[#]Equal contribution.

***Corresponding Authors**

*Dr. Trung-Dung Dang
School of Chemical Engineering, Hanoi University of Science and Technology, 1st Dai Co Viet, Hai Ba Trung, Hanoi, Vietnam
Fax: +84 43 868 0070 Tel: +84 43 868 0122
E-mail: dung.dangtrung@hust.edu.vn

*Prof. Arghya Narayan Banerjee
School of Mechanical Engineering, Yeungnam University, Gyeongsan, 712-749, South Korea
Fax: +82 53 810 2062 Tel: +82 53 810 2453
E-mail: arghya@ynu.ac.kr, banerjee_arghya@hotmail.com

*Prof. Sudipta Roy
Department of Chemical Engineering and Processing, University of Strathclyde, Glasgow, United Kingdom
Tel: 01415742371
E-mail: sudipta.roy@strath.ac.uk

ABSTRACT

By a simple wet-chemical procedure using a permanganate in the acidic medium, diatomite coated with amorphous manganese oxide nanoparticles was synthesized. The structural, microstructural and morphological characterizations of the as-synthesized catalysts confirmed the nanostructure of MnO_2 and its stabilization on the support - diatomite. The highly efficient and rapid degradation of methylene blue and methyl orange over synthesized MnO_2 coated Diatomite has been carried out. The results revealed considerably faster degradation of the dyes against the previously reported data. The proposed mechanism of the dye-degradation is considered to be a combinatorial effect of chemical, physicochemical and physical processes. Therefore, the fabricated catalysts have potential application in waste water treatment, and pollution degradation for environmental remediation.

Keywords: Diatomite; Permanganate; Manganese oxide; Methylene Blue, Methyl Orange; Rapid Degradation.

1. INTRODUCTION

Dye from textile, printing industries and other commercial activities have been a focus of environmental remediation in the last two decades [1-3]. Dye-containing waste has been considered as an important source of water pollution because dyes are highly toxic, and coloured water is undesirable. In addition, some synthetic dyes are carcinogenic, and difficult to degrade [2].

Methylene Blue (MB) and Methyl Orange (MO) are two of the normal and popular dyes which were used in industry. MB belongs to the thiazine class of dyes. It has many uses in a range of different fields and used as a photosensitizer, an antioxidant, an antiseptic, a stain for fixed and living tissues. It is also used as an organic dye to colour cotton, wool, acrylic fibers and silk. However, it can result in permanent burns to the eyes of human and animals, nausea, vomiting, profuse sweating, mental confusion and methemoglobinemia [4].

MO is a good representative of aromatic azo (-N=N-), dyes, which constitute about half of the total world dye market. Azo dyes are also a major class of synthetic organic compounds released by many industries such as paper, plastic, leather, food, cosmetic and pharmaceutical industries. Among environmental pollutants, azo dyes including MO make up a significant component of organic pollutants in general. Furthermore, such compounds are recognized as potential carcinogens [1,3,5].

Due to these concerns a variety of research has been performed in recent years to degrade MO and MB from waste waters. Some physical methods have been tested without adding any material but using solar irradiation, ultrasonication or generation of radio frequency plasma in water solution [6]. But traditionally, functionalized and nanosized materials such as Na_2SO_3, MgO, ZnO, copper, silver doped ZnO, ferric tungsten or nanoscale zero-valent iron particles [3,7-11] etc. are added for degradation or decolorization of these dyes. The most popular catalyst for MO and MB degradation is TiO_2 nanomaterial, which are

used solely or with some additives like H_2O_2, under solar irradiation [1,2,12-16]. But the disadvantage of TiO_2 is that that the material is costly and being a large band-gap material, its photosensitivity is limited to the wavelengths below 400 nm, *i.e.* to the ultraviolet region only, which comprises less than 5% of the overall solar energy spectrum [17].

Therefore, attention has shifted to find new and cost-effective low-bandgap catalysts which function in the visible-light-driven region, thus expanding the solar photocatalysis into the visible portion of the solar radiation. In this respect, manganese oxide (MnO_2) and its composites are considered to be highly promising catalysts for dye degradation, due to their low bandgap (direct bandgap ~2 eV or less [18]). MnO_2 which are well known as a strong adsorbents of metal ions, is naturally found in soils, aquifers and sediment, and therefore cost-effective. In addition, MnO_2 can be synthesized using oxidation of Mn(II) in basic solution [19], oxidation by MnO_4^- [20], O_2, $K_2S_2O_8$, and H_2O_2 [21], or reduction of MnO_4^- using different routes [22-26].

In this study, a composite of amorphous MnO_2 and diatomaceous earth, prepared via a simple wet-chemical method, is used to catalytically degrade MB and MO at ambient conditions. Diatomaceous earth (so-called diatomite or bio-silica) is a non-metallic, highly porous, and chemically inert mineral, composed of skeletal remains of single-cell water plants [27]. Due to its microporous structure and chemical properties, diatomite has been widely used as filter [28], adsorbent [29-31], insulating material [32], energy storage [33-37] catalyst support and natural insecticide [36,37].

Diatomite and diatomite coated MnO_2 have been used to remove heavy metal and many coloured dyes from aqueous solution [38-41]. Methylene blue, reactive black and reactive yellow were removed by physicochemical process - adsorption by diatomite and crystalline MnO_2 (birnessite)-coated diatomite [42-44]. The mechanism for removal was either due to the insertion/intercalation of dye molecules within the inter-layer spacing of

super-lattice birnessite or the adsorption at the surface of manganese oxide-coated diatomite via charge transfer process.

However, for environmental applications, the degradation of these toxic compounds into non-toxic products is very important. There are some reports about the degradation of Rhodamine B (RhB) and an azo dye - acid orange (AO7) by using amorphous manganese oxide-coated diatomite [44,45]. In our previous study, we have presented the degradation of RhB via MnO_2-bio-silica nanocomposites [44]. The mechanism for removal is based on the production of hydroxyl radicals by the reduction of Mn(IV) to Mn(II), which can oxidize the organic dyes efficiently. In this work we have tested the ability of MnO_2/Diatomite to degrade two different types of dyes: Methylene Blue (MB) - Methyl Orange (MO). A novel mechanism of the degradation kinetics is proposed, which consists of a chemical, physicochemical and physical process. Most importantly, the dye degradation time is found to be comparatively shorter than the previous reports [45], indicating the high efficiency of the as-synthesized catalysts for organic waste management.

2. EXPERIMENTS

2.1. Synthesis of the Catalyst

The catalyst was synthesized using the following steps. At first, a solution of 0.1 M potassium permanganate (Sigma-Aldrich, 99%), was prepared using distilled water. A separate solution of 6.0 M hydrochloric acid (Sigma-Aldrich) was also prepared. Secondly, 1 g of diatomite (Sigma-Aldrich, used as received), was mixed in 10 mL potassium permanganate solution. Then 2 ml of 6.0 M HCl is added to this mixture drop-wise. After the mixture has been stirred at room temperature for 4 hours, amorphous manganese oxide (MnO_2) is formed on the diatomite, which is then separated, washed five times with DI water and then dried at room temperature for 48 hours. The approximate weight ratio of coating

material (MnO_2) on the surface of diatomite was 1.6. A separate set of process steps were carried out without adding any diatomite. In this case amorphous MnO_2 was precipitated from the solution. This is referred to as "control" MnO_2, and was used to compare the performance of manganese oxide coated diatomite (MOCD). The detail of the synthesis process is furnished elsewhere [44].

2.2. Characterization

The control MnO_2, uncoated- and MnO_2- coated diatomite are characterized by x-ray powder diffraction (XRD) using a D8 Advance–Bruker X-ray diffractometer with Cu-K_α radiation (40 KV, 30 mA) and a Lynx-eye position sensitive detector. Field emission scanning electron microscope (FESEM, JEOL JSM-7600F) and energy-dispersive X-ray spectroscopy (EDX) were utilized to characterize the surface morphology. A high-resolution transmission electron microscope (HRTEM, JEM - 2100F) at 200 KeV field emission electron gun in Schottky mode was employed to determine particle size. The surface areas of the samples were measured using a Brunauer, Emmett and Teller (BET) ASAP 2420 (Micromeritics) system.

2.3. Confirmation of Catalytic Activities

The catalytic activity of the as-prepared control MnO_2 and MOCD is studied in order to evaluate their effectiveness in degradation of Methylene Blue (MB) and Methyl Orange (MO) from aqueous solution at ambient conditions (room temperature ~ $25^{O}C$ and atmospheric pressure). Firstly, the 0.1 mM MO and 0.06 mM MB stock solutions are prepared by dissolving 0.033 g of MO and 0.02 g of MB in 1000 mL DI water and stirred for 30 mins. Then, 10 ml of the dye stock solutions are placed in 50 mL beakers followed by addition of the solid samples (catalysts).

A series of solid samples of 2.5; 5.0; 7.5; 10.0 and 12.5 milligrams was added to the stock solution, and then each mixture was stirred (in normal light) for 30 mins at ambient conditions (for catalysis) at a pH value of 5 and then allowed to settle for 10 mins. To get the optimized time for catalysis, the above-mentioned degradation experiment is conducted for different times and it was observed that the decolorization of the dyes (MB and MO) were finished at 30 mins. The mixtures were centrifuged twice at 3000 *rpm* for 10 mins to separate the catalyst from solution, and then the centrifuged solution (supernatants) was kept in the dark before further analysis using UV-VIS spectrophotometer (Agilent 8453, United State, HUST) to estimate the dye degradation performance. A separate set of dye degradation experiments with uncoated diatomite was not necessary because, it has been shown that bare diatomite did not degrade the color of dyes [44].

3. RESULTS

3.1 Catalyst Characterization

The SEM images of the uncoated and MOCD prepared by the process mentioned above are shown in Figure 1. The Figure 1a shows the structure of the uncoated diatomite which is high-porosity skeletal-remain of single-cell water plants. The surface morphology and high porosity of this bio-structure can be used as the template to cover other functional materials for diverse applications. Figure 1b shows the image of diatomite after the immobilization of the amorphous MnO_2. The thickness of the coated MnO_2 is controlled by changing the weight ratio of the coating material - $KMnO_4$ and the substrate - diatomite. The optimum ratio to get a uniform, smooth, and stable coating layer is found to be 1.6 which was reported previously [44]. Inset of 1(b) represent the magnified version of a single pore of diatomite coated with MnO_2. The images 1(d), (e) and (f) in turn show elemental mapping of Si, Mn and O in the MOCD sample which was shown in Figure 1c. It is observed that SiO_2 (diatomite) and MnO_2

are uniformity distributed. Although the pore diameter of the hole structure of the diatomite is slightly reduced but the porosity is sufficient to enable reactions to proceed on MOCD.

The morphology of the amorphous MnO_2 needs to be compared against the composite diatomite (MOCD). Inset of Figure 1b and Figure S1 (Supporting Information) reveal that the MnO_2 coating comprises of nanospheres of which form worm-like fibers at the surface. The thickness of the worm-like fibers is approximately 10 nm and the structure is highly porous mainly because of the formation and release of the chlorine [44].

The nanostructures of the uncoated diatomite and the MOCD are shown in TEM images of Figure 2. The circular pores of uncoated diatomite (Figure 2a) are uniformly covered with amorphous MnO_2 nanoparticles (Figure 2b). The MnO_2 coats the inner surface of diatomite pores whilst retaining the porous structure of the diatomite. The HRTEM images and the SAED pattern in the Figure 2c and 2d show that the MnO_2 coating layer is dendritic and semicrystalline.

The Brunauer, Emmett and Teller (BET) surface area measurements are performed and the BET-N_2 adsorption-desorption curves, pore size distributions and BET plots are presented in Fig. S2 (Supporting data). Corresponding BET parameters are also given in Table S1 of the supporting data for comparison. The table revealed that uncoated diatomite had an average BET surface area of 2.60 m^2/g, vs. 126.28 m^2/g for amorphous MnO_2 nanopowder and 145.12 m^2/g for the MOCD composite, respectively. Clearly, MOCD samples offer the highest active surface area, which is due to the hybrid nanostructure of MOCD that leads to lesser total BJH pore volume against pure MnO_2.

Figure 3a represents the XRD traces of uncoated diatomite, control MnO_2, and MOCD. The XRD pattern of the diatomite agrees well with SiO_2 (JCPDS ICDD File Card # 00-001-0647) while the XRD pattern of the control amorphous MnO_2 is in agreement with the international crystallographic data (JCPDS ICDD File Card # 00-001-0649). The similar

nature of the XRD patterns of the control MnO_2 and the MOCD suggest that the surface of the substrate (diatomite) is uniformly covered. The EDX pattern (Figure 3b) of the uncoated diatomite reveals the presence of elemental Si and O (Si = 47.86 %; O = 51.55%). The EDX pattern of the MOCD (Figure 3c) shows Si, Mn, O and traces of K originating from the reactants during MnO_2 formation. Ions such as K^+ and H^+ (present in the solution during the MnO_2 formation reaction) could have been incorporated to balance the surface charge of the MnO_6 octahedra to stabilize the structure. These sites are considered to be very reactive and efficient in catalyzing the degradation of color dyes [46].

3.2 Catalyst Performance

The mixing of the MB solution with MOCD at room temperature resulted in a change in colour from blue → violet → pink → colorless, depending on the quantity of catalyst added. The digital images shown in the upper half of Figure 4(a) indicates the change in colour. With the highest amount of the catalyst (0.0125 g), the solution becomes almost colorless in less than 30 min. The UV-Vis spectra of the degraded dye solution also depict the decrement of the absorption peak with increase in the catalyst amount (lower half of Figure 4a), indicating efficient degradation of the MB solution. Generally, UV-Vis absorption spectra of the degraded dye solution shows maximum absorption (*i.e.* highest absorption peak) when the amount of dye within the solution is maximum. With increase in the catalysts amount the dye-degradation is increasing, which means the amount of dye within the solution is decreasing. Hence, UV-Vis abortion peaks are also decreasing with the increase in the catalyst amount.

The catalytic performances of the different added amounts of control MnO_2 and MOCD was analyzed by measuring the relative decrease in the dye concentration at

subsequent time against the initial value by estimating the peak absorbance of the absorption spectra of the dye solution according to the relation [47]:

$$\%\, d = \left(1 - \frac{a_{dye}^{\tau}}{a_{dye}^{0}}\right) X\ 100 \qquad (1)$$

where, % d is the percentage relative dye degradation, a_{dye}^{0} and a_{dye}^{τ} are the peak absorbance of dye solution at initial concentration and after catalysis over time τ, respectively. In this case, the results were shown in Figure 4b, where the relationship between the increment of catalyst and the decrement of the color dye - MB in the aqueous solution can be observed in detail. Both control MnO_2 and MOCD composites indicate considerable degradation of the MB dye solution, with MOCD having superior catalytic activity over control MnO_2 with similar Mn^{+4} concentration. The average difference of the catalytic performance between MOCD and control MnO_2 is 20% higher for the former. An obvious reason for this is the porous morphology of the host diatomite matrix, which offers much higher reactive surfaces for hydroxyl radical formation, as clearly depicted by the BET surface area measurements furnished above, and therefore, better degradation of the dye solution.

In this study, the catalytic ability for organic dye degradation of MOCD is not only tested with Methylene Blue (MB) - a thiazine class color dye but also with Methyl Orange (MO) - an azo class color dye. The decolorization of MO by the MOCD composite is shown in the digital images given in the upper half of Figure 5(a), whereas the degradation measurements in terms of UV-Vis absorption curves are furnished in the lower half of Figure 5(a). For comparison, MO solution is degraded with control MnO_2 too, with similar Mn^{+4} concentrations as MOCD composites.

In a similar way, the analysis of the catalytic performances of control MnO_2 and MOCD, as a function of different added amounts of catalysts into MO solutions, was performed using equation 1, and the data are furnished in Figure 5(b), which shows better catalytic performance of MOCD composites over control MnO_2, apparently because of the higher reactive surfaces of the porous diatomite matrix, as described for the MB degradation case.

4. DISCUSSIONS

The catalytic activity of uncoated diatomite is also tested in a similar way, but the previous data revealed that bare diatomite had insignificant efficiency in the degradation of color dyes [44]. This is because, under the operating experimental conditions, the natural pH of the diatomite solution is around 5 (mild acidic) and the surface charge of diatomite is approximately zero, and hence, there is no considerable attraction between the diatomite surface and color dyes [41,48]. Generally, the ionic dyes are removed via a surface adsorption mechanism, under very high (> 11) or very low (< 3) pH values, through electrostatic interaction between surface charge of the diatomite and ionized dye molecules [41,48]. Therefore, unless the diatomite solution is extremely acidic or alkaline, the dye removal would be insignificant. That is the reason the diatomite surface is coated with MnO_2 nanoparticles to produce strong oxidizing radicals within the dye solution, which chemically degrade the toxic dyes into non-toxic products, whereas, the porous structure of diatomite provides higher active surface area for better surface reactions. Hence, dye removal process via MOCD composite is basically a physicochemical process.

The proposed mechanism for this catalytic process is based on two subsequent processes: (i) the changing in the oxidation state of manganese in aqueous solution and

corresponding generation of strong oxidizing hydroxyl radical (OH^*) at some pH less than 7. This is because Mn^{IV} (which is the dominant oxidation state of Mn in our amorphous oxide nanostructures) are readily converted to Mn^{+2} state under pH < 7 to produce hydroxyl radicals (OH*) according to the following overall reaction schemes [44,49]:

$$\tfrac{1}{2}\, Mn^{IV}O_2\,(s) + 2H^+ + 2e^- \leftrightarrow \tfrac{1}{2}\, Mn^{+2}(aq.) + 2\, OH^* + H_2O \quad (E^O = +1.23\ V) \qquad (2)$$

(where E^O is the standard reduction potential). (ii) The newly generated hydroxyl radicals then oxidize the toxic organic dye efficiently and produce the non-toxic inorganic products via some intermediates as follows [44]:

OH* + toxic organic dyes → organic hydroxylated intermediates → CO_2 + H_2O + degraded non-toxic inorganic products (3)

More precisely, the formation of hydroxyl radicals (equation 2 can be explained by the generation of Mn^{IV}-HOH precursor complex; followed by the electron transfer to reduce Mn^{+4} to Mn^{+2} and subsequently release hydroxyl radicals as follows [49]:

A) Formation of precursor complex : $\tfrac{1}{2}Mn^{IV} + 2HOH \leftrightarrow (\tfrac{1}{2}\, Mn^{IV}, 2HOH)$ (4)

B) Transfer of electron : $(\tfrac{1}{2}\, Mn^{IV}, 2HOH) \leftrightarrow (\tfrac{1}{2}\, Mn^{II}, 2OH^*) + 2H^+$ (5)

C) Release of hydroxyl radical: $(\tfrac{1}{2}\, Mn^{II}, 2OH^*) \leftrightarrow \tfrac{1}{2}\, Mn^{II} + 2OH^*$ (6)

D) Release of reduced Mn^{II}: $\tfrac{1}{2}\, Mn^{II} \leftrightarrow \tfrac{1}{2}\, Mn^{+2}$ (7)

A closer look into the UV-Vis absorption curves in Figure 4(a) depicts that the absorption peaks are blue-shifted with respect to the reference curve of stock dye solution. This shift of the UV-Vis absorption peaks along with the change in the color of the dye solution are considered to be due to the degradation of the MB. The structure of MB includes the $C\text{-}S^+\text{=}C$

functional group and the OH^* can attack this group (inset of Fig. 4a). Therefore, the initial step of MB degradation is ascribed to the cleavage of the bond of the $C\text{-}S^+\text{=}C$ functional group [15] according to the following reaction:

$$R\text{-}S^+\text{=}R' + OH^* \rightarrow R\text{-}S(\text{=}O)\text{-}R' + H^+ \quad (8)$$

After that, the sulfoxide group can be attacked by OH^* to form the definitive dissociation of the two benzoic rings. Then, a series of reactions occurs to get hydroxyhydroquinone as the last aromatic compound before the opening of the ring. After the aromatic ring opening, the oxidation of OH^* continuously occurs to get the final products such as CO_2, H_2O and non-toxic inorganic compounds. The above-mentioned series of reactions produce various organic intermediates such as Azure A, B and C as well as semi-reduced MB, which have absorption maxima in the range of 625-635 nm, 648-655, 608-622 nm and 420 nm, respectively. The formation of these intermediates causes the blue shifting of the peak position (with respect to the initial MB absorption ~ 660 nm) as well as the changing of the color of the dye solution [7,15].

The mechanism of the catalysis of MO using control MnO_2 and MOCD is similar to that shown for MB situation (equation 2 and 3) [1,14]. A closer look into the UV-Vis absorption curves of MO solutions (Figure 5a) depicts that the main absorption peak of the stock MO dye solution is blue-shifted only slightly (unlike MB degradation case) from 465 nm to 450 nm, whereas the color of the MO dye changes naturally from dark orange to light orange and to almost colorless with the increment of catalyst. Generally, there are at least nine possible types of intermediates formed during the degradation of MO via demethylation, methylation and hydroxylation processes [50,51]. Each of these intermediates has different effect on the shifting of the absorption peak. Some of these tend to blue-shift the peak, whereas the others tend to red-shift the absorption peak. Therefore, due to these two

competing trends, the overall peak-shift becomes very small (or near-insignificant) in the current case.

It is noteworthy that, as compared to the previous reports [11,15,50,51], the current case reports almost two to four times faster catalytic performance of MOCD for MB and MO degradations. Such a faster catalysis process is not only manifested by the higher active surfaces provided by the porous diatomite matrix, but also affected by some secondary effects, as described below. The HRTEM images of MnO_2 (Figure 2c and 2d) depict the hairy structures, which contain small regions of crystalline domains at the edges of this catalyst. The analysis of SAED patterns of the hairy structure in the inset of the Figure 2d and crystallographic data indicate that the crystal structure resembles with the birnessite phase of crystalline MnO_2. Since the percentage of these crystalline domains is much smaller than the bulk of the amourphous MnO_2, the XRD signal only depicts the amorphous nature of the material. Therefore, these layer-structures of the superlattice birnessite MnO_2 at the edges of the coating layers manifests the intercalation of dye molecules within the octahedral layers to remove the dye. Thus, there are three simultaneous processes taking place during the dye degradation, such as, (i) conversion of Mn^{+4} to Mn^{+2} and the release of hydroxyl radicals to degrade the dye (chemical process), (ii) adsorption of dye within the inter-layer spacings of the small fraction of birnessite MnO_2 (physicochemical process) and (iii) higher surface reaction sites due to the porous diatomite matrix (physical process), to provide a rapid degradation/removal of MB and MO from aqueous solution.

It has already been discussed previously that under the applied experimental conditions with natural pH ~ 5, pure diatomite didn't show any adsorption of dye molecules. Since we have not changed the pH of the solution to extremely high (> 11) or extremely low (< 3) values, the dye decoloration process is primarily based on the catalytic degradation of

the dye solution via the change in the oxidation states of Mn in MnO_2, whereas a very small amount of dye intercalation at the layer structure of birnessite MnO_2 is taking place as the secondary effect, as stated above. Therefore, diatomite is basically used as a supporting matrix to deposit MnO_2 nanoparticles to provide high active surface area through the formation of MOCD nanohybrid. Hence, to analyze the kinetics of the catalytic process, we have firstly obtained the time effluence of the dye degradation curves for different catalytic amounts for both MOCD and pure MnO_2 and for both MB and MO degradations. Secondly, considering low dye concentrations in the current case, the catalytic degradation is modelled by pseudo first-order kinetic reaction, which also covers the adsorption properties of the catalyst surface, and expressed according to the following relation [52]:

$$-\ln\left[\frac{C_{dye}^{t}}{C_{dye}^{i}}\right] = \kappa_a t \tag{9}$$

where C_{dye}^{i} is the initial dye concentration and C_{dye}^{t} is the same at a degradation time t. κ_a is the pseudo first order rate constant. A plot of $-\ln\left[\frac{C_{dye}^{t}}{C_{dye}^{i}}\right]$ vs. t will be a straight line with the slope as κ_a. The above plots for the highest catalyst amount (0.0125 g) for MOCD (which is having highest degradation rate), and for both MB and MO degradations are given in Fig. S3 (Supporting data). The graph is fitted with a straight line with the value of κ_a around 0.14 to 0.15 min^{-1}. For other catalysts amounts, the graphs are similarly well-fitted with pseudo first order kinetic model. Recently, Zhang and co-authors [53] reported the catalytic degradation of Fe_2O_3@MnO_2 hybrid catalyst and showed that the degradation kinetics follow similar pseudo first order model with κ_a around 0.16 min^{-1}, which is comparable to our values.

Also to understand the relative influence of catalysts amount (both MOCD and MnO_2) on the dye degradations of both MB and MO, a relative degradation rate is obtained by considering the relative percentage degradation over a certain amount of time. The data are presented in Table S2 of Supporting Information. Clearly, 0.0125 g of MOCD and MnO_2 catalysts (per 10 ml of dye stock solution) showed maximum degradation rates. Apparently, an increase in the degradation rate with the increase in the catalysts amount is due to an increase in the number of active sites on the catalysts available for the reaction, which in turn increases the rate of radical formation [54]. But, with further increase in the catalysts amount, the degradation rate is observed to be decreased (not shown here), which is due to the agglomeration trend of the surplus amount of catalysts that retards the absorption/desorption equilibrium of the dye molecules on the catalysts surface and prevents uniform suspension of the catalysts for efficient catalysis.

To further corroborate the proposed dye removal mechanism in terms of catalytic degradation as primary process, and dye adsorption as the secondary process, the solid samples (MOCD catalysts) were collected after catalytic performance via centrifugation and separation from the dye solution (MB), and then imaged under SEM (as shown in Figure S4 of the Supporting Information). The MnO_2 coating is still observed on the surface of the diatomite, indicating good stability of the catalysts. However, compared to the image of the MOCD before dye degradation (Figure 1b), slight change in the morphology of the MOCD catalyst is observed after dye degradation. The magnified image (Fig. S4b) revealed that the porous surface of the MnO_2 layer is slightly smoothed out in some places, indicating the surface adsorption of the dye molecules. Qualitatively, this morphological change is found to only 10% against the entire porous surface. On the other hand, EDX analysis of the solid samples (MOCD catalysts) before and after dye degradation depicted almost 15% decrement in the elemental Mn within the coating layer after dye degradation process. This observation

clearly indicates that the primary catalytic process is the degradation via the conversion of solid Mn^{+4} into water soluble Mn^{+2} during chemical catalyzation (as explained above in Eqs. 2-7), whereas, dye adsorption is only the secondary process.

The stability and the regeneration ability are crucial concerns with regard to the practical application of the catalyst. The SEM micrographs of MOCD catalysts after the catalytic process (Fig. S4) clearly demonstrates uniform coating of MnO_2 layer on the diatomite surface, with the morphology scarcely changed, indicating good stability of the catalysts. Additionally, a low temperature (450^oC) heat treatment of the catalysts depicted the removal of the adsorbed organic species, without collapsing of the MOCD structure. Further usage of the recovered catalysts in successive catalytic cycles showed very good catalytic efficiency, indicating excellent stability, very good regeneration ability and prominent re-usability [55].

5. CONCLUSIONS

This study has presented the rapid degradation of a thiazine class dye - methylene blue and an azo class dye - methyl orange, under the presence of MnO_2-coated Diatomite. The MOCD composite catalyst is produced via a wet-chemical method under ambient conditions. Both control MnO_2 and MOCD show very good catalytic activity, and with the assistance of them, the degradation rate of MB and MO was promoted considerably, shortening the degradation time to as low as 30 min or less. With respect to control MnO_2, MOCD composite shows much better catalytic activity, mainly because of three simultaneous processes, such as (a) a chemical process, where hydroxyl radicals are formed via the reduction of Mn(IV) to Mn(II) which consequently degrade the dye, (b) a physicochemical process, where dye molecules are intercalated within the layered structure of birnessite MnO_2

to remove the dye from aqueous solution, and (c) a physical process, where higher active surface sites are provided by the porous matrix of the diatomite support to manifest greater surface reactions. Thus the material and method have potential applications in the field of waste water treatment, water splitting and pollution degradation.

Acknowledgements: This work is funded by Vietnam's National Foundation for Science and Technology Development (NAFOSTED) (Project Nr. 103.02-2013.76). We thanks for the supporting from British Council and Newton Fund-Researcher Links Travel Grant. We also thank Professor S.W. Joo of School of Mechanical Engineering, Yeungnam University for insightful discussions.

References

[1] L. Yu, J. Xi, M. D. Li, H. T. Chan, T. Su, D. L. Phillips and W. K. Chan, Phys. Chem. Chem. Phys. 14, 3589 (2012)

[2] M. Salehi, H. Hashemipour and M. Mirzaee, American J. Environ. Eng. 2, 1 (2012)

[3] Y. H. Shih, C. P. Tso and L. Y. Tung, J. Environ. Eng. Manage. 20, 137 (2010)

[4] L. Zhang, Y. Nie, C. Hu and X. Hu, J. Hazard. Mater. 190, 780 (2011)

[5] S. D. Gakakakar and A.V. Salker, Indian J. Chemical Tech. 16, 492 (2009)

[6] I. Miyamoto, T. Maehara, H. Miyaoka, S. Onishi, S. Mukasa, H, Toyota, M. Kuramoto, S. Nomura and A. Kawashima, J. Plasma Fusions Res. Series 8, 627 (2009)

[7] M. A. Tabbara and M. M. El Jamal, J. the University of Chemical Technology and Metallurgy 47, 275 (2012)

[8] Ch. Girginov, P. Stefchev, P. Vitanov and Hr. Dikov, J. Eng. Sci. Tech. Rev. 5, 14 (2012)

[9] S. B. Gajbhiye, Inter. J. Modern Eng. Res. 2, 1204 (2012)

[10] R. Rahimi, J. Shokrayian and M. Rabbani, 17th Inter. Electronic Conference on Synthetic Organic Chemistry Proceeding, DOI: 10.3390/ecsoc-17-b018

[11] A. Ameta, R. Ameta and M. Ahuja, Sci. Revs. Chem. Commun. 3, 172 (2013)

[12] X. T. Zhou, H. B. Ji and X. J. Huang, Molecules 17, 1149 (2012)

[13] K. Bubacz, J. Choina, D. Dolat and A. W. Morawski, Polish J. of Environ. Stud. 19, 685 (2010).

[14] M. N. Rashed and A. A. El-Amin, Inter. J. Phys. Sciences. 2, 73 (2007)

[15] A. Houas, H. Lachheb, M. Ksibi, E. Elaloui, C. Guillard and J. M. Herrmann, Appl. Catal. B Env. 31, 145 (2001)

[16] S. S. Al-Shamali, Australian J. Basic and Applied. Sci. 7, 172 (2013)

[17] U. Diebold, Surf. Sci. Rep. 48, 53 (2003)

[18] B. A. Pinaud, Z. Chen, A. N. Abram and T. F. Jaramillo, J. Phys. Chem. C 115, 11830 (2011)

[19] D. C. Golden, C. C. Chen and J. B. Dixon, Science 231, 717 (1986)

[20] J. Luo and S. L. Suib, Chem. Commun. 11, 1031 (1997)

[21] J. Moon, M. Awano, H. Takagi and Y. Fujishiro, J. Mater. Res. 14, 4594 (1999)

[22] J. Cai, J. Liu and S. L. Suib, Chem. Mater. 14, 2071 (2002)

[23] M. A. Cheney, S. W. Joo, A. N. Banerjee and B. K. Min, J. Colloid Interface Sci. 379, 141 (2012)

[24] M. A. Cheney, R. Jose, A. N. Banerjee, P. K. Bhowmik, S. Qian and J. M. Okoh**,** J. Nanomaterials Vol. 2009, ID 940462 (2009)

[25**]** M. A. Cheney, P. K. Bhowmik, S. Moriuchi, M. Villalobos, S. Qian and S.W. Joo, J. Nanomaterials Vol. 2008, ID 168716 (2008)

[26] M. A. Cheney, P. K. Bhowmik, S. Qian, S. W. Joo, W. Hou and J. M. Okoh, J. Nanomaterials Vol. 2008, ID 763706 (2008)

[27] K. R. Engh, *in Kirk-Othmer Encyclopedia of Chemical Technology* edited by M. Howe-Grant, Wiley, New York (1993) Vol. 8, p.108.

[28] E. I. El-Shafey, M. L. F. Gameiro, P. F. M. Correia and J. M. R. De Carvalho, Sep. Sci. Technol. 39, 3237 (2004).

[29] A. Ridha, H. Aderdour, H. Zineddine, M.Z. Benabdallah, M. El Morabit and A. Nadiri, Ann. Chim. Sci. Mater. 23, 161 (1998)

[30] S. Aytas, S. Akyil, M. A. A. Aslani and U. Aytekin, J. Radioanal. Nucl. Chem. 240, 973 (1999)

[31] K. Agdi, A. Bouaid, A. M. Esteban, P. F. Hernando, A. Azmani and C. Camara, J. Environ. Monit. 2, 420 (2000)

[32] A. N. Christensen, B. Lundtoft and I. C. Madsen, J. Am. Ceram. Soc. 84, 878 (2001)

[33] Z. Q. Wen, M. Li, F. Li, S. J. Zhu, X. Y. Liu, Y. X. Zhang, T. Kumeria, D. Losic, Y. Gao, W. Zhang and S. X. He, Dalton Trans. 45, 936 (2016)

[34] Y. X. Zhang, M. Huang, F. Li. X. L. Wang and Z Q. Wen. J. Power Sour. 246, 449 (2014)

[35] F. Li, Y. Xing, M. Huang, K. L. Li, T. T. Yu, Y. X. Zhang and D. Losic, J. Mater. Chem. A 3, 7855 (2015)

[36] E. Alvarez, J. Blanco, P. Avila and C. Knapp, Catal. Today 53, 557 (1999)

[37] Z. Korunic, J. Stored Prod. Res. 34, 87 (1998)

[38] Y. S. Al-Degs, M. A. M. Kharaisheh and M. F. Tutunji, Water Res. 35, 3724 (2001)

[39] Y. X. Zhang, X. D. Hao, F. Li, Z. P. Diao, Z. Y. Guo and J. Li, Industrial Eng. Chem. Res. 53, 6966 (2014)

[40] M. A. Al-Ghouti, Y. S. Al-Degs, M. A. M. Khraisheh, M. A. Ahmad and S. J. Allen, J. Environ. Manag. 90, 3520 (2009)

[41] M. A. Al-Ghouti, M. A. M. Khraisheh, S. J. Allen and M. N. Ahmad, J. Environ. Manag. 69, 229 (2003)

[42] M. A. Khraisheh, M. A. Al-Gouti, M. N. Ahmad and S. J. Allen, Water Environ. Res. 79, 51 (2004)

[43] M. A. Al-Ghouti, M. A. M. Khraisheh, M. A. Ahmad and S. J. Allen, J. Hazad. Mater. 146, 316 (2007)

[44] T. D. Dang,; A. N. Banerjee, M. A. Cheney, S. Qian,S. W. Joo and B. K. Min, Colloids Surf. B. 106, 151 (2013)

[45] A. Khataee, S. Bozorg, B. Vahid, T. D. Dang, Y. Hanihefpour and S. W. Joo, Current Nanoscience 11, 129 (2015)

[46] A. Nasser, G. Sposito and M. A. Cheney, Colloids Suf. A 163, 117 (2000)

[47] A. N. Banerjee, S. W. Joo, and B. M. Kim, J. Nanomaterials Vol. 2012, ID 201492 (2012)

[48] Y. Aldegs, M. A. M. Khraisheh and M. F. Tutunji, Water Res. 35, 3724 (2001)

[49] A. T. Stone, Environ. Sci. Technol. 21, 979 (1987)

[50] Y. Su, Y. Yang, H. Zhang, Y. Xia, Z. Wu, Y. Jiang, N. Fukuta, Y. Bando and Z. L. Wang, Nanotechnology 24, 295401 (2013)

[51] K. Dai, H. Chen, T. Peng, D. Ke and H. Yi, Chemosphere 69, 1361 (2007)

[52] N.A. Laoufi, D. Tassalit, F. Bentahar, Global NEST J. 10, 404 (2008).

[53] S. Zhang, Q. Fan, H. Gao, Y. Huang, X. Liu, J. Li, X. Xu, and X. Wang, J. Mater. Chem. A 4, 1414 (2016).

[54] H. Benhebal, M. Chaib, T. Salmon, J. Geens, A. Leonard, A. D. Lambert, M. Crine, B. Heinrichs, Alexandra Engineering Journal 52, 517 (2013).

[55] M. Hu, K. S. Hui and K. N. Hui, Chem. Eng. J. 254, 237 (2014)

Figure captions

Figure 1. SEM images of diatomite (a); MOCD under permanganate-to-diatomite weight ratio (ρ) of 1.6 (b, c) and the elemental mapping (d: Si mapping, e: Mn mapping, f: O mapping). Inset of (b) represents the magnified image of a single diatomite pore covered with MnO_2.

Figure 2. TEM images of diatomite (a); and MOCD under permanganate-to-diatomite weight ratio (ρ) of 1.6 (b). HRTEM images and SAED pattern of the hairy parts of MOCD at two different magnifications (c, d).

Figure 3. (a) XRD patterns of diatomite; control MnO_2; and MOCD; EDX patterns of diatomite (b) and MOCD (c).

Figure 4. (a) The digital photographs of Methylene Blue dye solution at different amount of catalysts to show color change due to catalytic degradation of MB and UV-vis adsorption spectra of catalytically degraded MB solution treated with MOCD. Inset shows the molecular structure of MB. (b) Material influence on catalytic degradation of MB dye using control MnO_2 and MOCD.

Figure 5. (a) The digital photographs of Methyl Orange dye solution at different amount of catalysts to show color change due to catalytic degradation of MO and UV-vis adsorption spectra of catalytically degraded MO solution treated with MOCD. Inset shows the molecular structure of MO. (b) Material influence on catalytic degradation of MO dye using control MnO_2 and MOCD

List of Figures

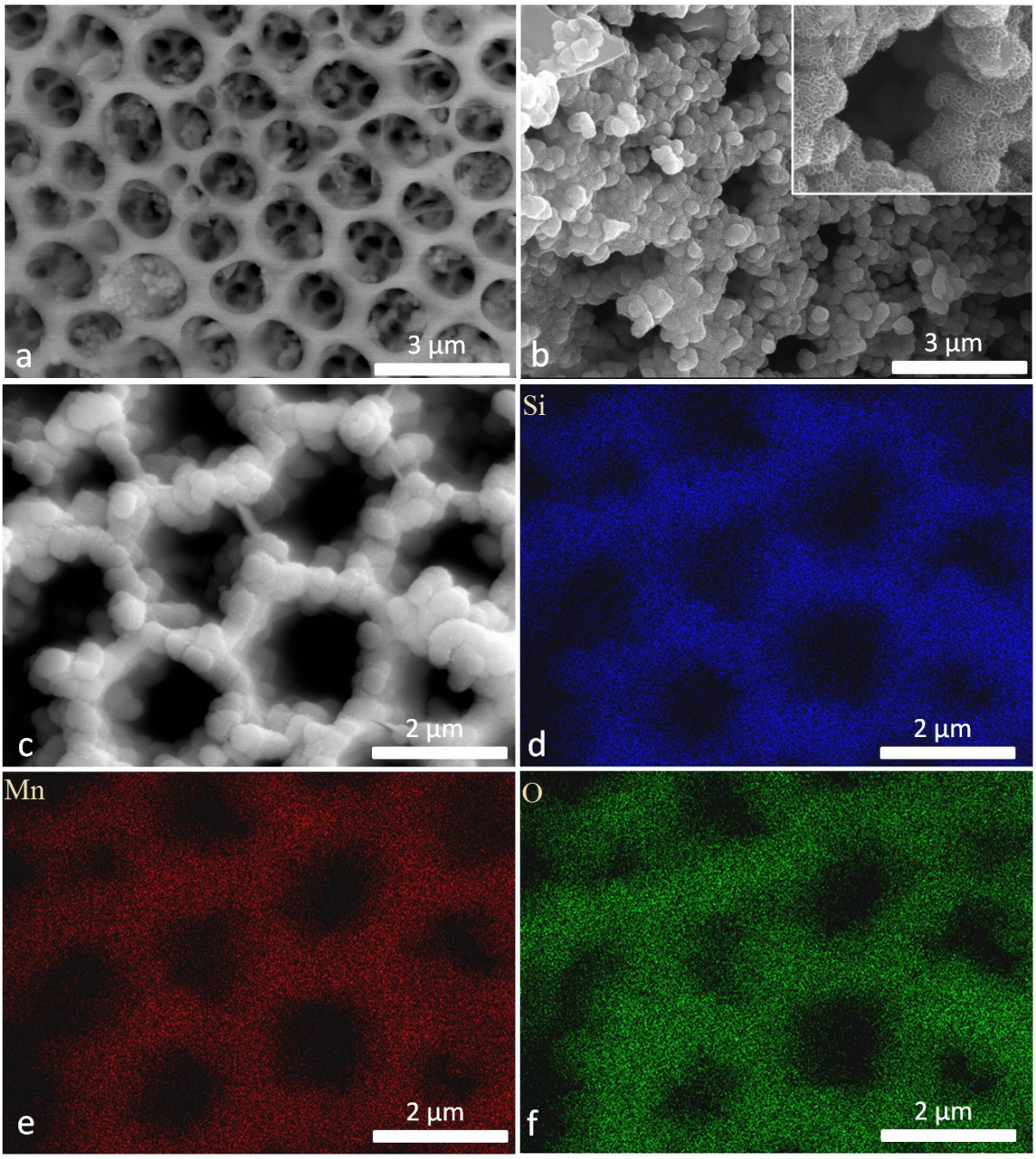

Figure 1.

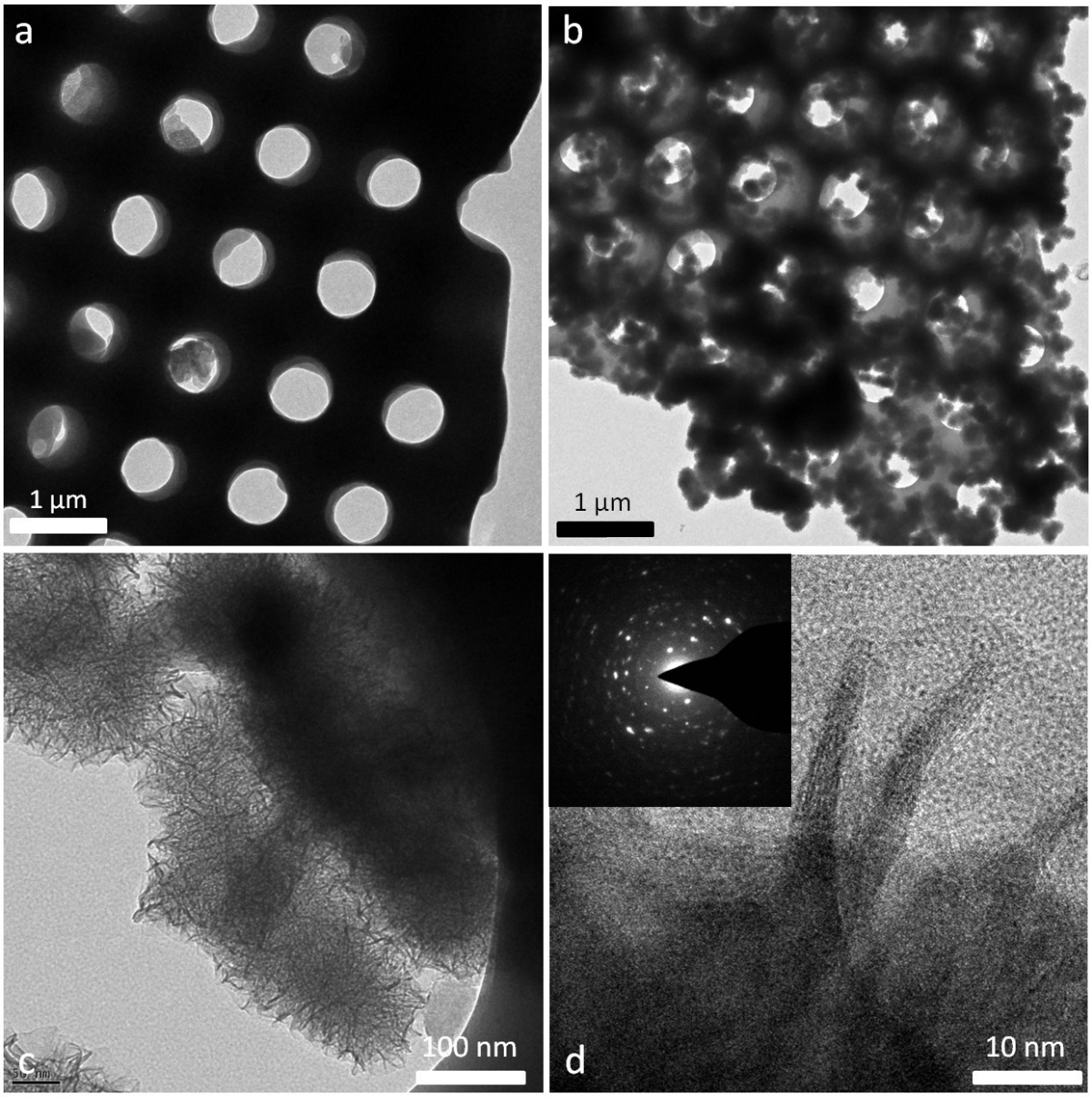

Figure 2.

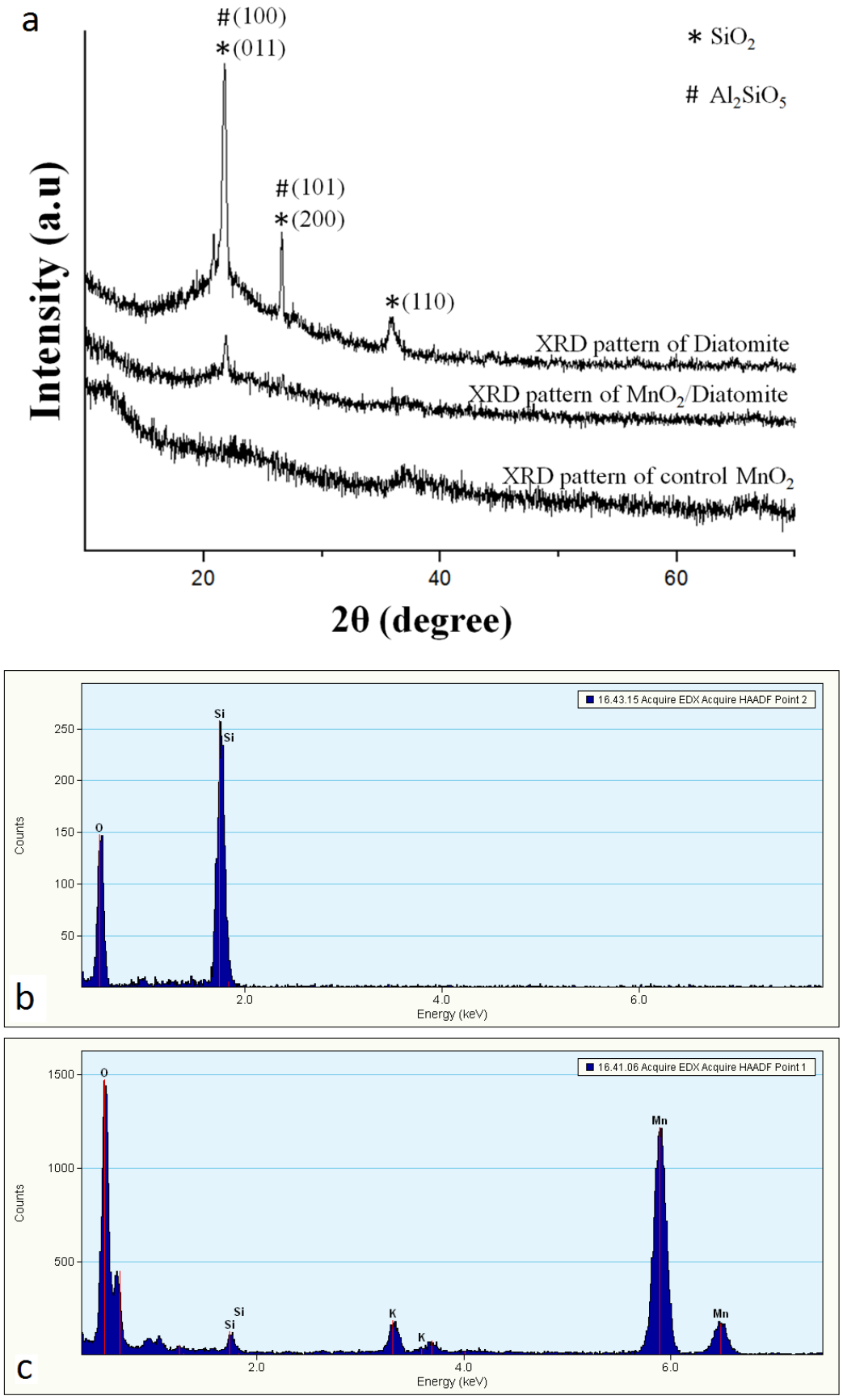
a
#(100)
*(011)
* SiO2
# Al2SiO5
#(101)
*(200)
*(110)
Intensity (a.u)
XRD pattern of Diatomite
XRD pattern of MnO2/Diatomite
XRD pattern of control MnO2
20
40
60
2θ (degree)
16.43.15 Acquire EDX Acquire HAADF Point 2
Si
Si
O
Counts
250
200
150
100
50
2.0
4.0
6.0
Energy (keV)
b
16.41.06 Acquire EDX Acquire HAADF Point 1
O
Mn
1500
1000
500
Counts
Si
Si
K
K
Mn
2.0
4.0
6.0
Energy (keV)
c

Figure 3.

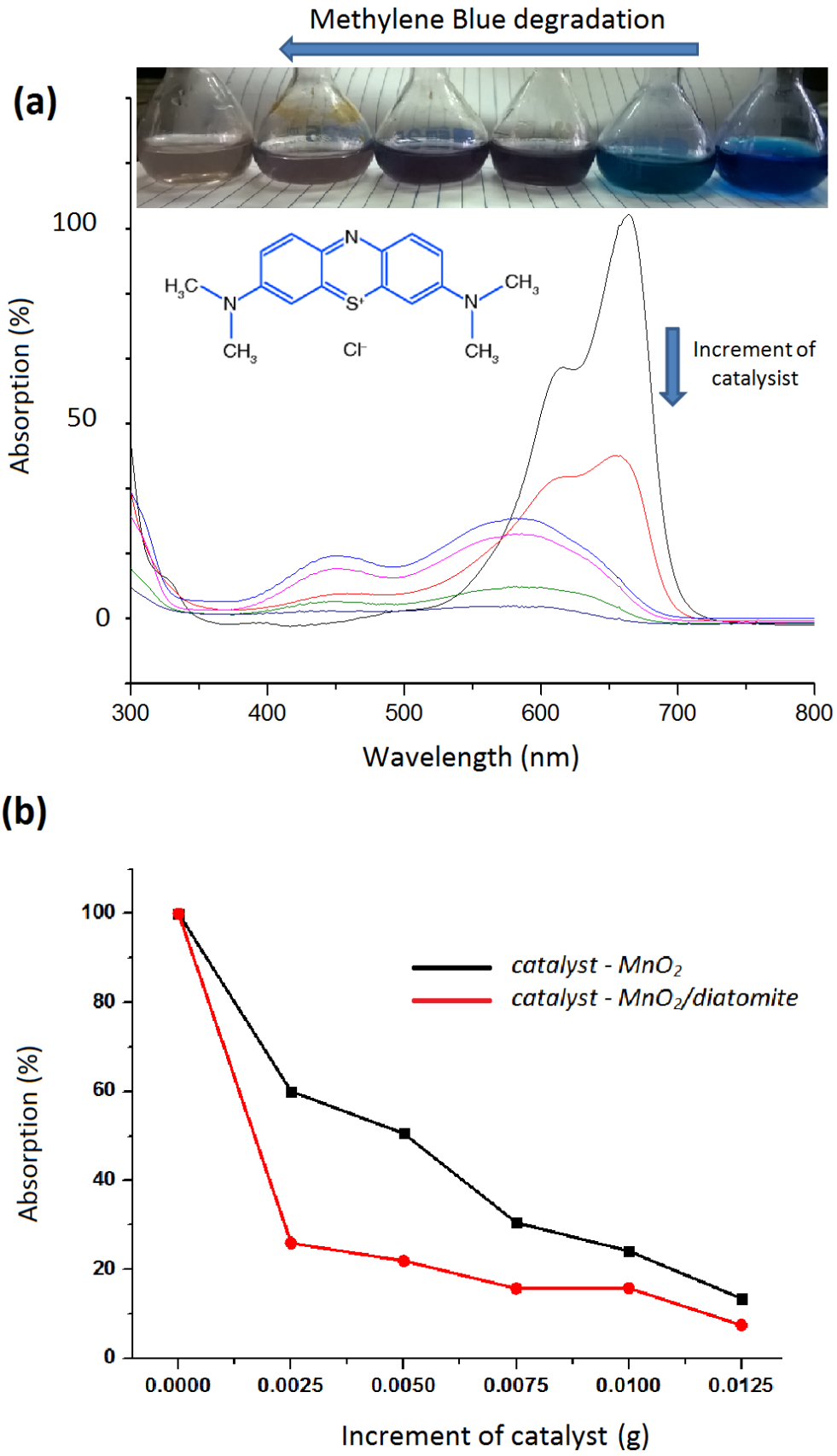
(a)
Methylene Blue degradation
Absorption (%)
100
50
0
300
400
500
600
700
800
Wavelength (nm)
Increment of catalysist
(b)
Absorption (%)
100
80
60
40
20
0
0.0000
0.0025
0.0050
0.0075
0.0100
0.0125
Increment of catalyst (g)
catalyst - MnO2
catalyst - MnO2/diatomite

Figure 4.

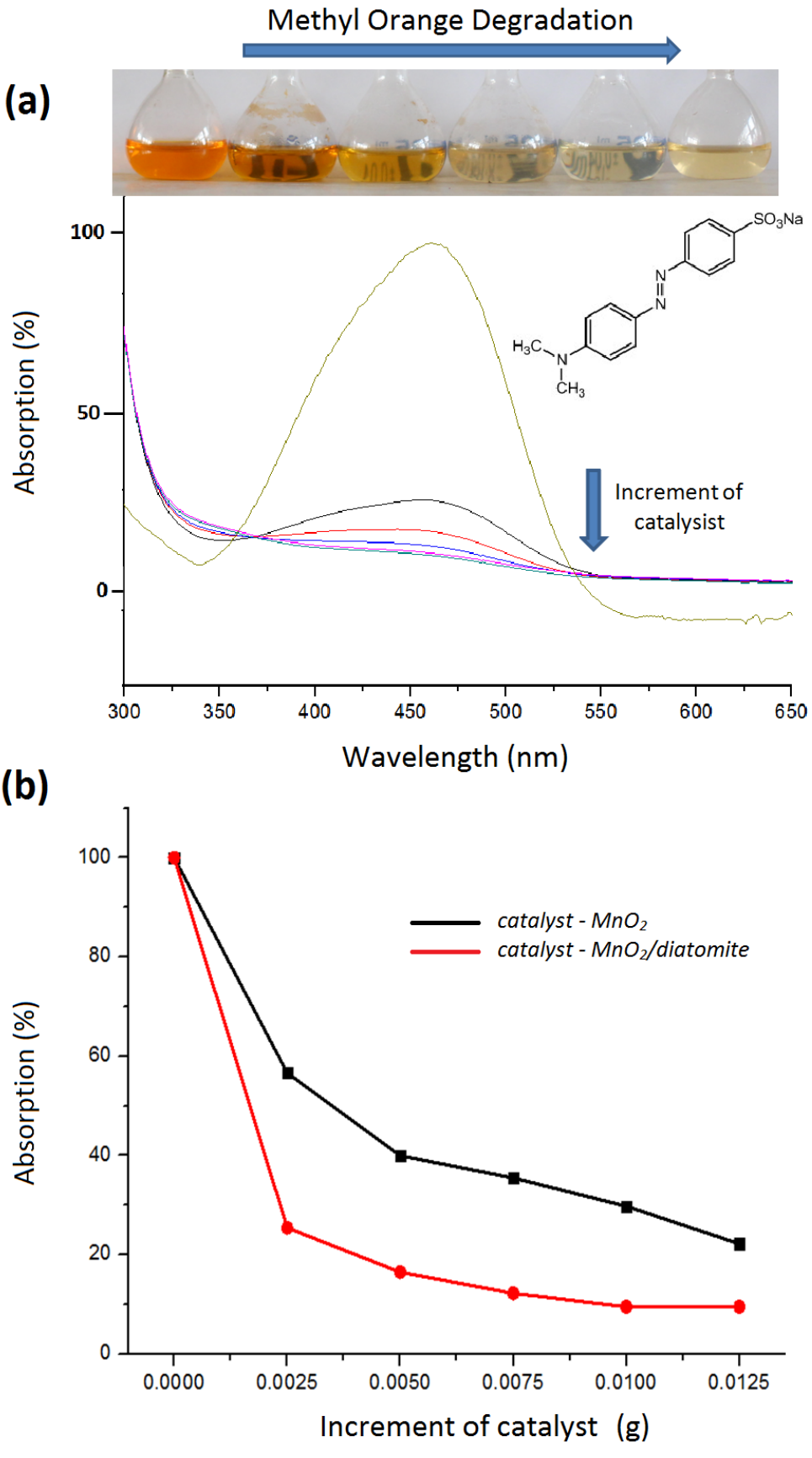
(a)
Methyl Orange Degradation
Absorption (%)
100
50
0
300
350
400
450
500
550
600
650
Wavelength (nm)
Increment of catalysist
SO3Na
H3C
N
CH3
(b)
Absorption (%)
100
80
60
40
20
0
0.0000
0.0025
0.0050
0.0075
0.0100
0.0125
Increment of catalyst (g)
catalyst - MnO2
catalyst - MnO2/diatomite

Figure 5.